Eur. Phys. J. A **13**, 69–74 (2002)

THE EUROPEAN PHYSICAL JOURNAL A

Frontiers and challenges of the nuclear shell model

T. Otsuka[1,2], Y. Utsuno[3], R. Fujimoto[1], B.A. Brown[4], M. Honma[5], and T. Mizusaki[6]

[1] Department of Physics, University of Tokyo, 7-3-1 Hongo, Bunkyo-ku, Tokyo 113-0033, Japan
[2] RIKEN, 2-1 Hirosawa, Wako-shi, Saitama 351-0198, Japan
[3] Japan Atomic Energy Research Institute, Tokai, Ibaraki, 319-1195, Japan
[4] National Superconducting Cyclotron Laboratory, Michigan State University, East Lansing, MI 48824, USA
[5] Center for Mathematical Sciences, University of Aizu, Tsuruga, Ikki-machi, Aizu-Wakamatsu, Fukushima 965-8580, Japan
[6] Department of Law, Senshu University, Higashimita, Tama, Kawasaki, Kanagawa, 214-8580, Japan

Received: 1 May 2001

Abstract. Two recent developments of the nuclear shell model are presented. One is a breakthrough in computational feasibility owing to the Monte Carlo Shell Model (MCSM). By the MCSM, the structure of low-lying states can be studied with realistic interactions for a wide, nearly unlimited basically, variety of nuclei. The magic numbers are the key concept of the shell model, and are shown to be different in exotic nuclei from those of stable nuclei. Its novel origin and robustness will be discussed.

PACS. 21.60.Cs Shell model – 21.30.Fe Forces in hadronic systems and effective interactions – 13.75.Cs Nucleon-nucleon interactions (including antinucleons, deuterons, etc.) – 21.10.-k Properties of nuclei; nuclear energy levels

1 Introduction

We present two recent developments in the nuclear shell model. One is a drastic change of the feasibility of the shell model calculations due to the Monte Carlo shell model. We will discuss on this point first by showing several examples. The other is more fundamental: new magic numbers in exotic nuclei. In exotic nuclei far from the β stability line, some usual magic numbers disappear while new ones arise. This is a very intriguing problem, and its mechanism is related to basic properties of nucleon-nucleon interaction in a very robust way. The second part of this report is on this very exciting and newest development.

2 Monte Carlo shell model

2.1 Outlook

The nuclear shell model has been started by Mayer and Jensen in 1949 [1] as a single-particle model. Afterwards, many valence particles are treated in the shell model, which then became a many-body theory or calculational method. A good example can be found in the *sd* shell [2]. The nuclear shell model has been successful in the description of various aspects of nuclear structure, partly because it is based upon a minimum number of natural assumptions, and partly because all dynamical correlations in the model space, beyond the mean-field calculations, can be incorporated appropriately. Although the direct diagonalization of the Hamiltonian matrix in the full valence-nucleon Hilbert space is desired, the dimension of such a space is too large in many cases, preventing us from performing the full calculations. Indeed, the shell model dimension is large, and the actual calculation becomes very difficult. By recent (conventional) shell model codes like ANTOINE by Caurier [3], VECSSE by Sebe [4] or MSHELL by Mizusaki [5], one can handle up to shell model dimension $\sim$ 100 million at technical edge, while practical calculations up to a few tens million dimension can be done.

Although the conventional shell model calculation has thus been developed significantly, the dimension can be much larger in many real nuclei and is indeed much beyond the reach of the future development. For instance, certain unstable nuclei being studied require calculations with more than 1 billion dimension. This is already very far beyond the limit of the existing conventional shell model codes.

In order to overcome those difficulties, one has to introduce an alternative approach. That is stochastic methods to many-body problems. We now turn to this subject.

The Shell Model Monte Carlo (SMMC) method has been proposed first [6], but it turned out that the SMMC is not very suitable for investigating level structure or transitions between eigenstates, partly due to the so-called minus-sign problem.

The Quantum Monte Carlo Diagonalization (QMCD) method has been proposed several years later by Honma,

Mizusaki and myself [7]. In the QMCD method, we select only basis states important to the eigenstate to be obtained. We then diagonalize the Hamiltonian matrix in a good approximation with those important bases [8–11]. The application of the QMCD method to the nuclear shell model is called the Monte Carlo Shell Model (MCSM). There have been several publications already on such applications [12–17], some of which are mentioned in this report.

2.2 Features of MCSM

There are two major advantages in the MCSM calculations. The first one is the feasibility of including many single-particle states. Because of this, one can describe drastic excitations within a nucleus. For instance, one can describe spherical yrast states, deformed rotational band and nearly superdeformed band at the same time with the same Hamiltonian in the same model space. This example is shown in refs. [10,12,17] where those three kinds of states are nicely presented by MCSM calculations with the full pf shell and the $g_{9/2}$ orbit. One finds quite good agreement with experiment [18]. This kind of description over a wide variety of states may be characterized as the feasibility along the energy axis. The yrast states and (normally) deformed band can be described basically within the pf shell [10,12], while the $g_{9/2}$ orbit is needed for the description of 16^+_1 and 18^+_1 states and negative-parity states. In fact, these states show quite large deformation, in particular, 16^+_1 and 18^+_1 [17].

The second major advantage of the MCSM calculation is the feasibility of handling many valence particles. The maximum number of valence particles is rather limited in the conventional calculations. However, if one wants to describe a long chain of isotopes entering the region of exotic nuclei far from the β stability line, the number of particles should change significantly. So, this capability plays an indispensable role in studying the structure of such exotic nuclei. This feature can be characterized as the feasibility along the isospin axis.

The second advantage is essential also in a recent work for describing the spherical-deformed phase transition in heavy nuclei, because the phase transition occurs as a function of the valence nucleons [14].

In exotic nuclei, two major shells are mixed rather often, and states of various characters arise at low energy. Even the ground state can be of quite exotic nature. In this situation, the above two feasibilities combined together play really crucial roles in clarifying the structure of exotic nuclei far from the β stability line. As an example, we shall discuss the structure of nuclei in the vicinity of ^{32}Mg in the next subsection.

2.3 Exotic nuclei around ^{32}Mg

The Monte Carlo shell model has been applied to the structure study of extremely neutron-rich unstable nuclei around ^{32}Mg [13]. Since the major issue is the breaking

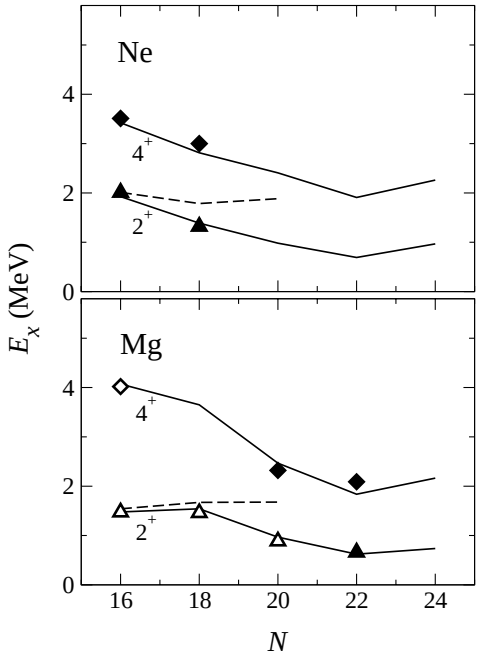

Fig. 1. Excitation energies of 2^+_1 and 4^+_1 states of even-A Ne and Mg isotopes obtained by MCSM calculation compared with experiment. Symbols are experimental data, while open symbols are those before the calculation of [13] and closed symbols are those after the calculation. Dashed lines are results of calculations within the sd shell.

of the $N = 20$ closed shell, one has to include both the sd shell and the pf shell. In fact, the effective shell gap is reported to become smaller near $Z = 10$ [13], and therefore intruder configurations come down and are mixed with normal configurations. The intruder configurations come down because they are more deformed and can gain more $T = 0$ correlation energies the large part of which is quadrupole deformation energy. A large deformation can be expected for Mg and Ne isotopes. All these mechanisms are combined and produce intriguing properties [13,19–21, 3,22–24].

The model space taken here consists of the full sd shell and the lower part of the pf shell (*i.e.*, $f_{7/2}$ and $p_{3/2}$). This space seems to be sufficiently large up to Si isotopes with the neutron number N, up to around 24. The effective interaction consists of three parts: i) the sd shell part is taken from the USD interaction [2], ii) the pf shell part is from the KB interaction [25], iii) the cross shell part is taken from [26] which was based upon the MK interaction [27].

Figure 1 shows MCSM results for excitation energies of the first 2^+ and 4^+ states of even-A Ne and Mg isotopes, exhibiting a nice agreement to experiment stretched up to $N = 22$ [28,22–24]. One sees in fig. 1, as a function of the neutron number, N, a sudden drop of the first 2^+ level both in experiment and MCSM sd-pf calculation, whereas the calculation within the sd shell shows a continuous increase. This difference clearly demonstrates the importance of the calculation including both sd and pf shells [19–21,3].

3 Magic numbers of exotic nuclei

3.1 Motivation

The magic number is the most fundamental quantity governing the nuclear structure. The nuclear shell model has been started by Mayer and Jensen by identifying the magic numbers and their origin [1]. The study of nuclear structure has been advanced on the basis of the shell structure associated with the magic numbers. This study, on the other hand, has been made predominantly for stable nuclei, which are on or near the β stability line in the nuclear chart. This is basically because only those nuclei have been accessible experimentally. In such stable nuclei, the magic numbers suggested by Mayer and Jensen remain valid, and the shell structure can be understood well in terms of the harmonic-oscillator potential with a spin-orbit splitting.

Recently, studies on exotic nuclei far from the β stability line have started owing to development of radioactive nuclear beams. The magic numbers in such exotic nuclei can be a quite intriguing issue. We shall show that new magic numbers appear and some others disappear in moving from stable to exotic nuclei in a rather novel manner due to a particular part of the nucleon-nucleon interaction.

3.2 Effective single-particle energies

In order to understand underlying single-particle properties of a nucleus, we can make use of *effective (spherical) single-particle energies (ESPEs)*, which represent mean effects from the other nucleons on a nucleon in a specified single-particle orbit. The two-body matrix element of the interaction depends on the angular momentum J, coupled by two interacting nucleons in orbits j_1 and j_2. Since we are investigating a mean effect, this J-dependence is averaged out with a weight factor $(2J+1)$, and only diagonal matrix elements are taken. Keeping the isospin dependence, $T = 0$ or 1, the so-called monopole Hamiltonian is thus obtained with a matrix element [29,13]:

$$V^T_{j_1 j_2} = \frac{\sum_J (2J+1)\langle j_1 j_2 | V | j_1 j_2 \rangle_{JT}}{\sum_J (2J+1)}, \quad \text{for } T = 0,\ 1, \quad (1)$$

where $\langle j_1 j_2 | V | j_1' j_2' \rangle_{JT}$ stands for the matrix element of a two-body interaction, V.

The ESPE is evaluated from this monopole Hamiltonian as a measure of mean effects from the other nucleons. The normal filling configuration is used. Note that, because the J-dependence is taken away, only the number of nucleons in each orbit matters. As a natural assumption, the possible lowest isospin coupling is assumed for protons and neutrons in the same orbit. The ESPE of an *occupied* orbit is defined to be the separation energy of this orbit with the opposite sign. Note that the separation energy implies the minimum energy needed to take a nucleon out of this orbit. The ESPE of an *unoccupied* orbit is defined to be the binding-energy gain by putting a proton or neutron into this orbit with the opposite sign.

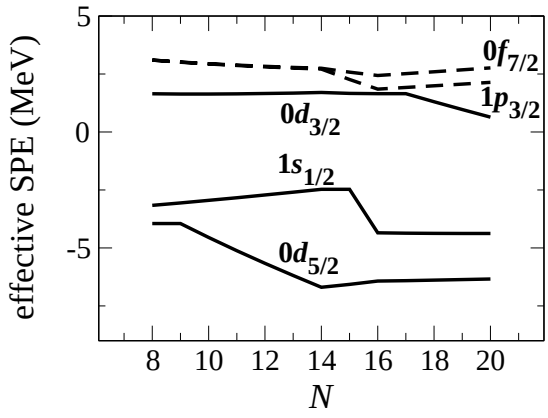

Fig. 2. Effective single-particle energies of neutrons of O isotopes.

3.3 Shell gap at N = 16

In fig. 2, ESPEs are shown for O isotopes. The Hamiltonian and the single-particle model space are the same as those used in [13], where the structure of exotic nuclei with $N \sim 20$ has been successfully described within a single framework. Between $N = 9$ and 14, the $0d_{5/2}$ comes down due to the attractive monopole contribution: $V^{T=1}_{0d_{5/2}0d_{5/2}}$ in eq. (1). The origin of this attraction is certainly the strongly attractive pairing. The same mechanism works for the $1s_{1/2}$ between $N = 15$ and 16. Beside the (monopole) pairing, the $T = 1$ interaction is quite weak, and produces even slightly repulsive effect on the ESPEs, as can be seen clearly in fig. 2. For instance, from $N = 9$ up to 15, the $1s_{1/2}$ goes up, because neutrons are filling $0d_{5/2}$ (in the normal filling approximation) and $V^{T=1}_{0d_{5/2}1s_{1/2}} > 0$.

A significant gap is found at $N = 16$ with the energy gap between the $0d_{3/2}$ and $1s_{1/2}$ orbits equal to about 6 MeV. This is a quite large gap comparable to the gap between the *sd* and *pf* shells in ^{40}Ca. The neutron number $N = 16$ should show features characteristic of magic numbers as pointed out by Ozawa *et al.* [30] for observed binding-energy systematics. A figure similar to fig. 2 was shown in [31] for the USD interaction [2], while only nuclei with subshell closures were taken. Basically because the $0d_{3/2}$ orbit has positive energy as seen in fig. 2, O isotopes heavier than ^{24}O are unbound for the present Hamiltonian in agreement with experiments [32,33], whereas the $0d_{3/2}$ orbit has negative energy for the USD interaction [31].

As discussed above, the gap between $0d_{5/2}$ and $1s_{1/2}$ increases gradually, ending up with a sizable gap at $N = 14$. Since neutrons start to occupy the $1s_{1/2}$ at $N = 15$ in the normal filling scheme, this gap can be seen also in the binding-energy systematics [34]. The 2^+ level of ^{22}O has been observed [35] in agreement with the shell model calculation [13] where the same Hamiltonian is used as for the ESPEs in fig. 2. Thus, the $N = 14$ gap between $1s_{1/2}$ and $0d_{5/2}$ is more related to the monopole component of the pairing-dominated $T = 1$ interaction within the $0d_{5/2}$ orbit. This work is, however, concerned with an-

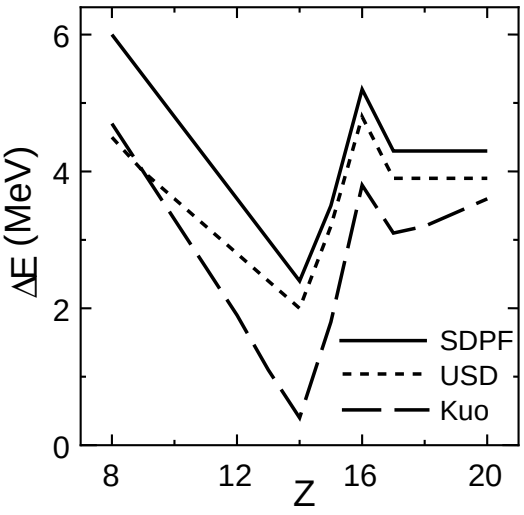

Fig. 3. Effective $1s_{1/2}$-$0d_{3/2}$ gap in $N = 16$ isotones as a function of Z. Shell model Hamiltonians, SDPF, USD and "Kuo" are used. See the text.

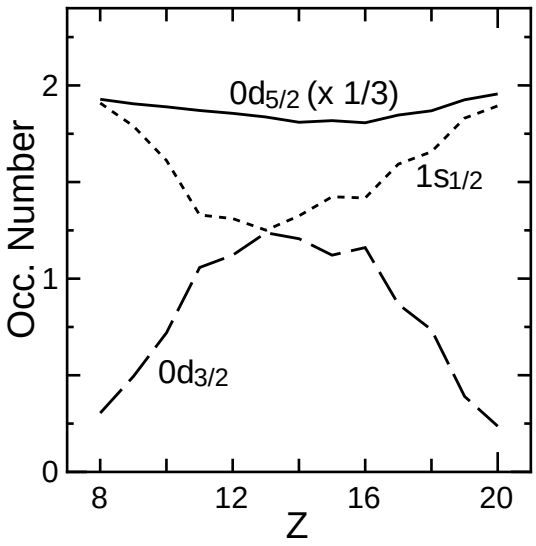

Fig. 4. Occupation numbers of *sd* shell orbits for neutrons in $N = 16$ isotones as a function of Z.

other magic structure at $N = 16$, presenting its origin in more fundamental levels and significance in a broader scope.

One finds that the gap between the $0d_{3/2}$ and $1s_{1/2}$ orbits is basically constant within a variation of $\sim \pm 1$ MeV. In lighter O isotopes, valence neutrons occupy predominantly $0d_{5/2}$ and this gap does not make much sense to the ground or low-lying states. The gap becomes relevant to those states only for $N > 14$. Thus, the large $0d_{3/2}$-$1s_{1/2}$ gap exists for O isotopes in general, while it can have major effects on the ground state for heavy O isotopes, providing us with a magic nucleus ^{24}O at $N = 16$.

Figure 3 shows the effective $0d_{3/2}$-$1s_{1/2}$ gap, *i.e.*, the difference between ESPEs of these orbits, in $N = 16$ isotones with $Z = 8$–20 for three interactions: "Kuo" means a G-matrix interaction for the *sd* shell calculated by Kuo [36], and USD was obtained by adding empirical modifications to "Kuo" [2]. The present shell model interaction is denoted SDPF hereafter, and its *sd* shell part is nothing but USD with small changes [13]. Steep decrease of this gap is found in all cases, as Z departs from 8 to 14. In other words, a magic structure can be formed around $Z = 8$, but it should disappear quickly as Z deviates from 8 because the gap decreases very fast. The slope of this sharp drop is determined by $V^{T=0,1}_{0d_{5/2}0d_{3/2}}$ in eq. (1), where the dominant contribution is from $T = 0$.

The gap can be calculated from the Woods-Saxon potential. The resultant gap is rather flat, and is about half of the SDPF value for $Z = 8$.

The occupation number of the neutron $1s_{1/2}$ is calculated for the nuclei shown in fig. 3. Figure 4 shows the occupation numbers obtained with the USD interaction in the *sd* shell, while those obtained with the present SPDF Hamiltonian are very similar. This occupation number is nearly two for ^{24}O as expected for a magic nucleus, but decreases sharply as Z increases. It remains smaller (< 1.5) in the middle region around $Z = 14$, and finally goes up again for $Z \sim 20$. This means that the $N = 16$ magic structure is broken in the middle region of the proton *sd* shell, where deformation effects also contribute to the breaking. The $N = 16$ magic number is thus quite valid at both ends. It is of interest that the gap becomes large again for larger Z, due to other monopole components.

3.4 Shell structures of ^{30}Si and ^{24}O

We now discuss, in more detail, the sharp drop of the gap indicated in fig. 3 for Z moving away from 8. This drop is primarily due to the rapid decrease of the $0d_{3/2}$ ESPE for neutrons. Figure 5 shows ESPEs for ^{30}Si and ^{24}O, both of which have $N = 16$. Note that ^{30}Si has six valence protons in the *sd* shell on top of the $Z = 8$ core and is indeed a stable nucleus, while ^{24}O has no valence proton in the usual shell model. In fig. 5 (a), the neutron $0d_{3/2}$ and $1s_{1/2}$ are rather close to each other, while keeping certain gaps from the other orbits. Thus, the $0d_{3/2}$-$1s_{1/2}$ gap becomes smaller as seen in fig. 5 (a).

In fig. 5 (b), shown are ESPEs for an exotic nucleus, ^{24}O. The $0d_{3/2}$ is lying much higher, very close to the *pf* shell. A considerable gap ($\sim$ 4 MeV) is between the $0d_{3/2}$ and the *pf* shell for the stable nucleus ^{30}Si, whereas an even larger gap ($\sim$ 6 MeV) is found between $0d_{3/2}$ and $1s_{1/2}$ for ^{24}O. The basic mechanism of this dramatic change is the strongly attractive interaction shown schematically in fig. 5 (c), where $j_> = l + 1/2$ and $j_< = l - 1/2$ with l being the orbital angular momentum. In the present case, $l = 2$. One now should remember that valence protons are added into the $0d_{5/2}$ orbit as Z increases from 8 to 14. Due to a strong attraction between a proton in $0d_{5/2}$ and a neutron in $0d_{3/2}$, as more protons are put into $0d_{5/2}$, a neutron in $0d_{3/2}$ is more strongly bound. Thus, the $0d_{3/2}$ ESPE for neutrons is so low in ^{30}Si as compared to that in ^{24}O.

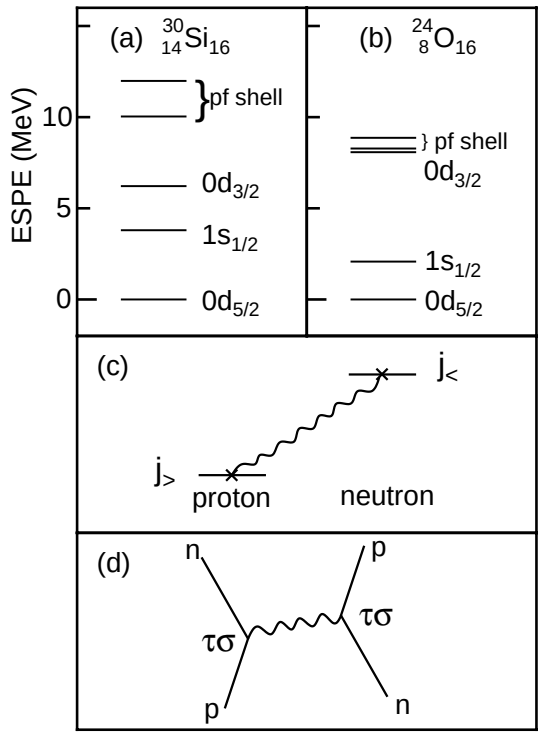

Fig. 5. ESPEs for (a) ^{30}Si and (b) ^{24}O, relative to $0d_{5/2}$. (c) Major interaction producing the basic change between (a) and (b). (d) Process relevant to the interaction in (c).

3.5 Spin-isospin dependence in NN interaction

The process illustrated in fig. 5 (d) produces the attractive interaction in fig. 5 (c). The NN interaction in this process is written as

$$V_{\tau\sigma} = \tau \cdot \tau \ \sigma \cdot \sigma \, f_{\tau\sigma}(r). \qquad (2)$$

Here, the symbol "$\cdot$" denotes a scalar product, τ and σ stand for isospin and spin operators, respectively, r implies the distance between two interacting nucleons, and $f_{\tau\sigma}$ is a function of r. In the long-range (or no r-dependence) limit of $f_{\tau\sigma}(r)$, the interaction in eq. (2) can couple only a pair of orbits with the same orbital angular momentum l, which are nothing but $j_>$ and $j_<$.

The σ operator couples $j_>$ to $j_<$ (and vice versa) much more strongly than $j_>$ to $j_>$ or $j_<$ to $j_<$. Therefore, the spin flip process is more favored in the vertexes in fig. 5 (d). The same mathematical mechanism works for isospin: the τ operator favors charge exchange processes. Combining these two properties, $V_{\tau\sigma}$ produces large matrix elements for the spin-flip isospin-flip processes: proton in $j_>$ $\rightarrow$ neutron in $j_<$ and vice versa. This gives rise to the interaction in fig. 5 (c). This feature is a general one and is maintained with $f_{\tau\sigma}(r)$ in eq. (2) with reasonable r-dependences.

Although $V_{\tau\sigma}$ yields sizable attraction between a proton in $j_>$ and a neutron also in $j_>$, the effect is weaker than in the case of fig. 5 (c).

In stable nuclei with $N \sim Z$ with ample occupancy of the $j_>$ orbit in the valence shell, the proton (neutron) $j_<$ orbit is lowered by neutrons (protons) in the $j_>$ orbit. In exotic nuclei, this lowering can be absent, and then the $j_<$ orbit is located rather high, not far from the upper shell. In this sense, the proton-neutron $j_>$-$j_<$ interaction enlarges a gap between major shells for stable nuclei with proper occupancy of relevant orbits.

The origin of the strongly attractive $V_{\tau\sigma}$ is quite clear. The One-Boson Exchange Potentials (OBEPs) for π and ρ mesons have this type of terms as major contributions. While the OBEP is one of major parts of the effective NN interaction, the effective NN interaction in nuclei can be provided by the G-matrix calculation with core polarization corrections. Such effective NN interaction will be called simply G-matrix interaction for brevity. The G-matrix interaction should maintain the basic features of meson exchange processes, and, in fact, existing G-matrix interactions generally have quite large matrix elements for the cases shown in fig. 5 (c) [37].

We would like to point out that the $1/N_c$ expansion of QCD by Kaplan and Manohar indicates that $V_{\tau\sigma}$ is one of three leading terms of the NN interaction [38]. Since the next order of this expansion is smaller by a factor $(1/N_c)^2$, the leading terms should have rather distinct significance.

3.6 Disappearance of N = 20 magic structure: Same origin

We now turn to exotic nuclei with $N \sim 20$. The ESPE has been evaluated for them in [13]. The small effective gap between $0d_{3/2}$ and the pf shell for neutrons is obtained, and is found to play essential roles for various anomalous features. This small gap is nothing but what we have seen for ^{24}O in fig. 5 (b). Thus, the disappearance of $N = 20$ magic structure in $Z = 9$–14 exotic nuclei and the appearance of the new magic structure in ^{24}O have the same origin: $V_{\tau\sigma}$.

3.7 Magic numbers in the p shell: N = 6 vs. N = 8

A very similar mechanism works for p shell nuclei. The neutron $0p_{1/2}$ orbit becomes higher as the nucleus loses protons in its spin-flip partner $0p_{3/2}$. The $N = 8$ magic structure then disappears, and $N = 6$ becomes magic, similarly to $N = 16$ magic number in sd shell. As a consequence, ^{8}He is well bound, whereas ^{9}He is not bound. This is analogous to the situation that ^{24}O is well bound, but ^{25}O is unbound.

3.8 Heavier nuclei: N = 34 etc.

Moving back to heavier nuclei, from the strong interaction in fig. 5 (c), we can predict other magic numbers, for instance, $N = 34$ associated with the $0f_{7/2}$-$0f_{5/2}$ interaction. In heavier nuclei, $0g_{7/2}$, $0h_{9/2}$, etc. are shifted upward in neutron-rich exotic nuclei, disturbing the magic numbers $N = 82$, 126, etc. It is of interest how the r-process of nucleosynthesis is affected by it.

3.9 Summary of the section

In summarizing this section, we showed how magic numbers are changed in nuclei far from the β stability line: $N = 6$, 16, 34, etc. can become magic numbers in neutron-rich exotic nuclei, while usual magic numbers, $N = 8$, 20, 40, etc., may disappear. Since such changes occur as results of the nuclear force, there is isospin symmetry that similar changes occur for the same Z-values in mirror nuclei. The mechanism of this change can be explained by the strong attractive $V_{\tau\sigma}$ interaction which has robust origins in OBEPs, G-matrix and QCD. In fact, simple structure such as magic numbers should have a simple and sound basis. Since it is unlikely that a mean central potential can simulate most effects of $V_{\tau\sigma}$, we should treat $V_{\tau\sigma}$ rather explicitly. It is nice to build a bridge between very basic feature of exotic nuclei and the basic theory of hadrons, QCD. In existing Skyrme HF calculations except for those with Gogny force, effects of $V_{\tau\sigma}$ may not be well enough included, because the interaction is truncated to be of δ-function type. The relativistic mean-field calculations must include pion degrees of freedom to be consistent with $V_{\tau\sigma}$. Thus, the importance of $V_{\tau\sigma}$ opens new directions for mean-field theories of nuclei. Loose-binding or continuum effects are important in some exotic nuclei. By combining such effects with those discussed in this talk one may draw a more complete picture for the structure of exotic nuclei. Finally, we would like to mention once more that the $V_{\tau\sigma}$ interaction should produce large, simple and robust effects on various properties, and may change the landscape of nuclei far from the β stability line in the nuclear chart.

The authors are very grateful to Professor M. Ishihara for his continuous interests and encouragements. In particular, it is deeply appreciated that Professor Ishihara has kept supporting the Alphleet computer system in RIKEN, with which many of MCSM calculations have been carried out. One of the authors (TO) ackowledges Professors K. Yazaki and T. Sebe for various collaborations. This work was supported in part by Grant-in-Aid for Scientific Research (A)(2) (10304019) from the Ministry of Education, Science and Culture.

References

1. M.G. Mayer, Phys. Rev. **75** 1969 (1949); O. Haxel, J.H.D. Jensen, H.E. Suess, Phys. Rev. **75** 1766 (1949).
2. B.A. Brown, B.H. Wildenthal, Annu. Rev. Nucl. Part. Sci. **38**, 29 (1988).
3. E. Caurier, F. Nowacki, A. Poves, J. Retamosa, Phys. Rev. C **58**, 2033 (1998).
4. A. Schmidt, I. Schneider, C. Friessner, A.F. Lisetskiy, N. Pietralla, T. Sebe, T. Otsuka, P. von Brentano, Phys. Rev. C **62**, 044319 (2000).
5. T. Mizusaki, RIKEN Accel. Prog. Rep. **33**, 14 (2000).
6. S.E. Koonin, D.J. Dean, K. Langanke, Phys. Rep. **278**, 1 (1997) and references therein.
7. M. Honma, T. Mizusaki, T. Otsuka, Phys. Rev. Lett. **75**, 1284 (1995).
8. T. Mizusaki, M. Honma, T. Otsuka, Phys. Rev. C **53**, 2786 (1996).
9. M. Honma, T. Mizusaki, T. Otsuka, Phys. Rev. Lett. **77**, 3315 (1996).
10. T. Otsuka, M. Honma, T. Mizusaki, Phys. Rev. Lett. **81**, 1588 (1998) and references therein.
11. T. Otsuka, T. Mizusaki, M. Honma, J. Phys. G **25**, 699 (1999).
12. T. Mizusaki, T. Otsuka, Y. Utsuno, M. Honma, T. Sebe, Phys. Rev. C **59**, R1846 (1999).
13. Y. Utsuno, T. Otsuka, T. Mizusaki, M. Honma, Phys. Rev. C **60**, 054315 (1999).
14. N. Shimizu, T. Otsuka, T. Mizusaki, M. Honma, Phys. Rev. Lett. **86**, 1171 (2001).
15. T. Mizusaki, T. Otsuka, M. Honma, B.A. Brown Phys. Rev. C **63**, 044306 (2001).
16. Y. Utsuno, T. Otsuka, T. Mizusaki, M. Honma, Phys. Rev. C **64**, 011301 (2001).
17. T. Mizusaki, T. Otsuka, M. Honma, B.A. Brown, in *Proceedings of RIKEN Symposium Shell Model 2000*, to be published in Nucl. Phys. A (2002).
18. D. Rudolph *et al.*, Phys. Rev. Lett. **82** (1999) 3763
19. E.K. Warburton, J.A. Becker, B.A. Brown, Phys. Rev. C **41**, 1147 (1990).
20. A. Poves, J. Retamosa, Phys. Lett. B **184**, 311 (1987); Nucl. Phys. A **571**, 221 (1994).
21. N. Fukunishi, T. Otsuka, T. Sebe, Phys. Lett. B **296**, 279 (1992).
22. D. Guillemaud-Mueller *et al.*, Nucl. Phys. A **426**, 37 (1984).
23. A. Azaiez *et al.*, in *Proceedings of the International Conference Nuclear Structure 98*, edited by C. Baktash, AIP Conf. Proc. Vol. **481** (AIP, New York, 1999) p. 243.
24. K. Yoneda *et al.*, Phys. Lett. B 499, 233 (2001).
25. T.T.S. Kuo, G.E. Brown, Nucl. Phys. A **114**, 241 (1968).
26. D.E. Alburger, J.A. Becker, B.A. Brown, S. Raman, Phys. Rev. C **34**, 1031 (1996).
27. D.J. Millener, D. Kurath, Nucl. Phys. A **255**, 315 (1975).
28. R.B. Firestone *et al.* (Editors), *Table of Isotopes* (Wiley, New York, 1996).
29. A. Poves, A. Zuker, Phys. Rep. **70**, 235 (1981).
30. A. Ozawa *et al.*, Phys. Rev. Lett. **84**, 5493 (2000).
31. B.A. Brown, Rev. Mex. Fis. **39**, Suppl. 2, 21 (1983).
32. D. Guillemaud Mueller *et al.*, Phys. Rev. C **41**, 937 (1990); M. Fauerbach *et al.*, Phys. Rev. C **53**, 647 (1996); O. Tarasov *et al.*, Phys. Lett. **409**, 64 (1997).
33. H. Sakurai *et al.*, Phys. Lett. B **448**, 180 (1999) and references therein.
34. G. Audi *et al.*, Nucl. Phys. A **624**, 1 (1997).
35. P.G. Thirolf *et al.*, Phys. Lett. B **485**, 16 (2000).
36. T.T.S. Kuo, Nucl. Phys. A **103**, 71 (1967).
37. M. Hjorth-Jensen, T.T.S. Kuo, E. Osnes, Phys. Rep. **261**, 125 (1995); M. Hjorth-Jensen, private communication.
38. D.B. Kaplan, A.V. Manohar, Phys. Rev. C **56**, 76 (1997).